COLD SPRING HARBOR
Molecular Case Studies

RESEARCH REPORT

9p21.3 Microdeletion involving *CDKN2A/2B* in a young patient with multiple primary cancers and review of the literature

Marlene Richter Jensen,[1] Ulrik Stoltze,[1,2] Thomas Van Overeem Hansen,[1,2] Mads Bak,[1] Astrid Sehested,[2] Catherine Rechnitzer,[2] René Mathiasen,[2] David Scheie,[3] Karen Bonde Larsen,[3] Tina Elisabeth Olsen,[3] Aida Muhic,[4] Jane Skjøth-Rasmussen,[5] Maria Rossing,[6] Kjeld Schmiegelow,[2,7] and Karin Wadt[1]

[1]Department of Clinical Genetics, [2]Department of Pediatrics and Adolescent Medicine, [3]Department of Pathology, [4]Department of Oncology, [5]Department of Neurosurgery, [6]Center for Genomic Medicine, Copenhagen University Hospital Rigshospitalet, Copenhagen 2100, Denmark; [7]Institute of Clinical Medicine, Faculty of Medicine, University of Copenhagen, Copenhagen 2100, Denmark

Abstract Germline pathogenic variants in *CDKN2A* predispose to various cancers, including melanoma, pancreatic cancer, and neural system tumors, whereas *CDKN2B* variants are associated with renal cell carcinoma. A few case reports have described heterozygous germline deletions spanning both *CDKN2A* and *CDKN2B* associated with a cancer predisposition syndrome (CPS) that constitutes a risk of cancer beyond those associated with haploinsufficiency of each gene individually, indicating an additive effect or a contiguous gene deletion syndrome. We report a young woman with a de novo germline 9p21 microdeletion involving the *CDKN2A/CDKN2B* genes, who developed six primary cancers since childhood, including a very rare extraskeletal osteosarcoma (eOS) at the age of 8. To our knowledge this is the first report of eOS in a patient with *CDKN2A/CDKN2B* deletion.

Corresponding author:
Karin.wadt@regionh.dk

Ontology terms: astrocytoma; cutaneous melanoma; neoplasm of the skin; neurofibromas; osteosarcoma

Published by Cold Spring Harbor Laboratory Press

doi:10.1101/mcs.a006164

[Supplemental material is available for this article.]

INTRODUCTION

CDKN2A and *CDKN2B*, both located on Chromosome 9p21, are involved in cell cycle regulation. *CDKN2A* encodes the tumor suppressors $p16^{INK4A}$ and $p14^{ARF}$ that regulate the cell cycle through the pRB and p53 pathways, respectively. *CDKN2B* encodes the protein $p15^{INK4B}$, which, along with $p16^{INK4A}$, acts as a cyclin-dependent kinase inhibitor and has been implicated in renal cell carcinoma predisposition in a single study (Jafri et al. 2015).

Pathogenic germline variants in *CDKN2A* are mainly associated with a risk of cutaneous melanoma that is more than 10-fold higher than the general population. Furthermore, *CDKN2A* variants affecting $p16^{INK4A}$ increase pancreatic cancer risk. Germline alterations in *CDKN2A* are also occasionally associated with a rare melanoma-astrocytoma syndrome, which predisposes to malignant melanomas and neural system tumors, including astrocytomas and meningiomas (Chan et al. 2017).

Because of their rarity, the significance of germline deletions involving both *CDKN2A* and *CDKN2B* is poorly described. Case reports of families or individuals with large deletions

involving both *CDKN2A* and *CKDN2B* (Table 1) have reported neurofibromas, giant cell tumors of bone and multiple primary cancers including sarcomas, such as a malignant peripheral nerve sheath tumor (Baker et al. 2016; Chan et al. 2016), thus clinically mimicking phenotypes of cancer predisposition syndromes such as neurofibromatosis type 1 (NF1) or Li–Fraumeni syndrome (LFS). We report a case of a 21-yr-old woman without significant family history of cancer, who developed six primary malignant tumors (extraskeletal osteosarcoma, lymphoepithelial carcinoma, low-grade myofibroblastic sarcoma, melanoma, anaplastic pleomorphic xanthoastrocytoma, and high-grade astrocytoma with piloid features) and 16 benign or premalignant tumors (Tables 2 and 3). Single-nucleotide polymorphism (SNP) array and whole-genome sequencing (WGS) identified a de novo germline microdeletion involving the entire *CDKN2A* and *CDKN2B* gene regions, previously published in an overview of childhood cancer cases (Østrup et al. 2018).

RESULTS

Clinical Presentation and Family History

At age 8 the proband, a previously healthy, nondysmorphic female with normal development, Iraqi heritage, and consanguineous parents, developed a swelling in her right upper arm. The tumor was biopsied, and histology, immunohistochemistry, and electron microscopy identified the tumor most likely to be an extraskeletal osteosarcoma (for histopathological description, view Table 2 footnotes). Treatment consisted of preoperative chemotherapy initially following the EpSSG NRSTS 2005 protocol (fosfamide, Adriamycin), without response, therefore altered with response to EURAMOS protocol (cisplatin, doxorubicin, and high-dose methotrexate) followed by resection and postoperative chemotherapy.

At age 13, she developed a swollen, painless lymph node next to the left ear. Resection of the lymph node showed a metastasis of an Epstein–Barr virus (EBV)-negative lymphoepithelial carcinoma. Tonsillectomy, adenoidectomy, and biopsies from nasopharynx, tongue root, and pharyngoepiglottic fold were unable to confirm the site of the primary tumor; however, the rhinopharynx was considered the most likely origin. A few months later, a relapse was identified adjacent to a resected lymph node and treated with radiation therapy of nasopharynx and the neck bilaterally (34 × 2 Gy, 6 F/W) and concomitant chemotherapy (cisplatin). In the diagnostic process of the lymphoepithelial carcinoma, a positron emission tomography/computes tomography (PET/CT) scan identified a process located in the right pelvis near the iliacus muscle. A 12-mo treatment follow-up scan showed slow growth. The pathology of an ultrasound-guided biopsy identified the process as a neurofibroma, which was completely and uneventfully resected. Pathological examination including immunohistochemistry of biopsy and resected tumor showed a tumor consisting of a single nodulus containing small spindle-shaped cells with regular oval nuclei and a normal staining pattern, showing no atypia, necrosis, or mitoses. Somatic genetic testing has not been performed, but pathology showed a classical pattern of neurofibroma. No café-au-lait spots or freckling were present, but the patient had multiple regular skin nevi throughout her body, including a Spitz nevus which was subsequently removed.

At age 15, the proband experienced severe headache, intermittent emesis, and paresthesia in the right parietal region. A brain magnetic resonance imaging (MRI) scan showed a large tumor in the right temporal lobe measuring ~25 × 17 mm. The tumor was surgically removed *in toto* and identified as an anaplastic pleomorphic xanthoastrocytoma (APXA), which was confirmed by genome-wide methylation analysis using the Heidelberg classifier (molecularneuropathology.org). The tumor showed a somatic *BRAF* mutation (p. Val600Glu) and loss of heterozygosity for the *CDKN2A/CDKN2B* gene region. Exome sequencing was performed, and all tumor-specific variants can be viewed in Table 4. No further

Table 1. Previous reports of *CDKN2A–CDKN2B* gene microdeletions

Case	Age at first malignant tumor	Clinical manifestations	Genomic analysis	Germline deletion	Family history
Petty et al. 1993	Not specified	By age 34: 8 melanomas, multiple atypical nevi, plexiform neurofibroma	FISH, Southern Blot, PFGE, PCR of STR polymorphisms	Unbalanced de novo cytogenic rearrangement of Chromosomes 5p and 9p, reported spanning at least 6 Mb of DNA; encompassing 2–3 Mb of Chromosome 9p	
Frigerio et al. 2014	10	Neurothekeoma, anaplastic astrocytoma, tectal mesencephalic lesion, 10 melanomas, neurofibroma	Microsatellite analysis, MLPA, aCGH	2.1 Mb (de novo), involving *MTAP, IFN* gene cluster, *FOCAD*, and partly *CDKN2B-AS1;* Seq(GRCh37) del(9)(p21.3) NC_00009.11: g.19934141-22069982del	Untested: Monozygotic twin sister with dysplastic nevi and slow growing cerebral lesion
Our case	8	Can be viewed in Tables 2 and 3	WGS, SNP array, MLPA	1.7 Mb (de novo); Seq(GRCh37) del(9)(p21.3) NC_00009.11: g.20657836-22353823del	
Baker et al. 2016	18 (proband's son)	Pontomedullary primitive neuroectodermal tumor	Whole-genome oligonucleotide array CGH, SNP array	At least 1.5 Mb, involving *MTAP* and partly *FOCAD*; Seq(GRCh37) del(9)(p21.3) NC_00009.11: g.20951885-22447709del; further, two CNVs of unknown significance and an amplification of unknown significance	Carriers (proband and proband's sister): neurofibromas, squamous papilloma, benign histiocytoma, melanoma, atypical nevi; eight untested family members: leukemia, chondrosarcoma, melanoma, cervical cancer, four members with unspecified cancer; noncarrier: melanomas, atypical nevi, lipoma
Chan et al. 2017	31	Pleomorphic xanthoastrocytoma, 2 diffuse astrocytomas, peripheral nerve sheath tumor	Targeted NGS of 479 cancer-associated genes, including selected introns	1.1 Mb, partly involving *MTAP*; Seq(GRCh38) del(9)(p21.3) NC_00009.11: g.21700000-22800000del	Untested family members: oral cancer (father, paternal uncle), glioblastoma (sister), melanoma (paternal uncle, grandfather), brain cancer (paternal grandfather)

(*Continued on next page.*)

Table 1. (*Continued*)

Case	Age at first malignant tumor	Clinical manifestations	Genomic analysis	Germline deletion	Family history
Pasmant et al. 2007; Bahuau et al. 1998	Not specified	Neural system tumors, melanomas	Bahuau et al.: heterozygosity mapping based on microsatellite markers Pasmant et al.: STS real-time PCR-based gene dose mapping, long-range PCR and nucleotide sequencing	403 kb; approximate coordinates: 9:21,926,315-22,329,545	13 confirmed carriers by Bahuau et al. (3 of which were tested by Pasmant et al.): a total of 8 melanomas, at least 6 neural system tumors, and 1 unspecified neoplasm
Chan et al. 2016	38	Laryngeal squamous cell carcinoma, high-grade malignant peripheral nerve sheath tumor	WGS, validated by qPCR	~270 kb; the deletion is partially truncating the flanking *MTAP* and *CDKN2B-AS*	Untested family members: giant cell tumor of bone (brother), possibly colon cancer (mother), possibly liver cancer (father)

(FISH) Fluorescence in situ hybridization, (PFGE) Pulsed-field gel electrophoresis, (PCR) polymerase chain reaction, (STR) short tandem repeat, (MLPA) multiplex ligation-dependent probe amplification, (aCGH) array comparative genomic hybridization, (WGS) whole-genome sequencing, (SNP) single-nucleotide polymorphism, (CNV) copy number variant, (NGS) next-generation sequencing, (STS) sequence-tagged sites, (qPCR) quantitative PCR.

treatment was given because of her, at this time, extensive chemotherapy and radiation exposure, including consideration of future treatment options, as the tumor was *BRAF* mutated. Remission lasted a year before a local relapse occurred. Once again, a complete surgical resection was performed with no further therapy added. In the same year, at age 17, a surveillance PET/CT scan showed increased FDG uptake in the right gastrocnemius muscle, reflecting a low-grade myofibroblastic sarcoma. Histopathological description can be viewed in the Table 2 footnotes, and histopathological images in Supplemental Figure S1. The tumor was surgically removed with clean resection margins. No further therapy was given.

At age 18, she was diagnosed with her fifth primary cancer, a superficial spreading malignant melanoma on her left shoulder with a tumor thickness of 1.3 mm. Sentinel node examination showed micrometastasis in one of two sentinel lymph nodes in the axillary region, and surgical resection was performed. The patient has Fitzpatrick skin phototype 4 and no record of sunburns in childhood. Further, there are no other known melanoma cases in her family.

In the same year, a brain surveillance MRI revealed an asymptomatic hypothalamic brain tumor. Following initial observation, progression of tumor size led to a biopsy being performed. Based on histology and genome-wide methylation analysis the tumor was classified as a high-grade astrocytoma with piloid features. Like the APXA, loss of heterozygosity for the *CDKN2A/CDKN2B* gene region was demonstrated. The high-grade astrocytoma with piloid features further showed a pathogenic and a likely pathogenic somatic mutation in the *NF1* gene (NM_000267.c.6789_6792del and NM_000267.c.1393-1G > A, respectively) and no somatic *BRAF* mutation was identified, supporting the diagnosis of a new primary tumor. Information regarding somatic analysis by next-generation sequencing (NGS) can be viewed in the Table 4 footnotes. Treatment of the second astrocytoma consisting of radiation (1.8 Gy × 30 F/54 Gy) and chemotherapy (temozolomide) was initiated. Evaluation after radiotherapy and two series temozolomide showed pseudoprogression of the tumor. Early follow-up scans (11 mo) show a stable tumor size (Fig. 1).

In addition to the six malignant tumors described above, the proband has had three premalignant atypical neurofibromas, all surgically resected, and 13 benign tumors since age

Table 2. Clinical manifestations and treatment of malignant and premalignant tumors in our proband

Age (y)	8	13	15	17	18			19	20	22
Diagnosis	Extraskeletal osteosarcoma[a]	Parotid metastasis of lymphoepithelial carcinoma	Anaplastic pleomorphic xanthoastrocytoma	Low-grade myofibroblastic sarcoma[a]	Relapse of APXA	Melanoma with micrometastasis in one axillary lymph node	High-grade astrocytoma with piloid features	Premalignant atypical neurofibroma (several tumors)	Premalignant atypical neurofibroma	Premalignant atypical neurofibroma[a]
Location	Right upper arm	Next to right ear	Right temporal lobe	Right gastrocnemius muscle	Right temporal lobe	Left shoulder	Left side of hypothalamus	Left brachial plexus	Left side of neck	Right neuroforamina, Th2-3
Symptoms	Swollen tumor	Swollen, painless lymph node	Headache, emesis, paresthesia in right parietal region	Asymptomatic	Asymptomatic	Change of color, pain	Asymptomatic	Swollen tumor	Swollen tumor	Asymptomatic
Preoperative imaging	Ultrasound, X-ray, MRI, PET/CT	Ultrasound, PET/CT	MRI, PET/CT	PET/CT, MRI, ultrasound	MRI	None	MRI, PET/CT	MRI	MRI	MRI
Preoperative biopsy	Yes	No	No	No	No	No	Yes	No	No	Biopsied ~2 yr before resection
Treatment	Preoperative chemotherapy, resection, postoperative chemotherapy	Resection, postoperative radiation therapy and chemotherapy	Resection	Resection	Resection	Resection, reresection, sentinel node with resection of 2 nodes	Radiation therapy, chemotherapy	Resection	Resection	Resection

(APXA) Pleomorphic xanthoastrocytoma, (MRI) magnetic resonance imaging, (PET/CT) positron emission tomography/computed tomography.
[a]Histopathological descriptions
Extraskeletal osteosarcoma (eOS): A mesenchymal tumor with no connection to the skeletal system consisting of very pleomorphic cells and osteoclast like giant cells. Without immunohistochemical features of specific differentiation. In the pretreatment biopsy there was identification of osteoid. In the posttreatment resection specimen, there was treatment response but no osteoid could be identified. The diagnosis of eOS therefore rests on the pretreatment biopsy, and the diagnosis of an undifferentiated pleomorphic sarcoma cannot be excluded.
Low-grade myofibroblastic sarcoma: A mesenchymal tumor consisting of infiltrative, cellular fascicles of myofibroblastic spindle cells with focal nuclear atypia. Immunohistochemistry with smooth muscle actin (SMA) and calponin positivity. Desmin was negative.
Atypical neurofibromatous neoplasms of uncertain biological potential (ANNUBP): A wavy spindle cell neoplasm with a variably myxoid to collagenous stroma (shredded carrots). There was some cytological atypia, areas with hypercellularity and mitosis (but no more than 2 mitosis/10 high-power field [HPF]). Immunohistochemistry was positive for S-100.

Table 3. Overview of benign tumors in our proband, including type of tumor, age, and location

Tumor type	Number of tumors	Age at diagnosis	Location
Neurofibromas	3	14	Pelvic region, right femoral nerve (resected)
		17	Left brachial plexus (resected)
			Peripheral nerve in right forearm (proximal and ulnar located) (resected)
Aneurismatic bone cyst	1	19	Right middle cranial fossa near the cavernous sinus (embolized)
Cellular neurothekeoma	1	20	Left side of neck (resected)
Benign soft tissue tumor	1	20	Left side of neck (resected)
Tumors identified radiologically without biopsy or resection	9	18	Intermuscular process in relation to right schiatic nerve near femur midshaft[a]
		19	In relation to left femoral nerve/femoral condyle[b]
		20	Left cerebellopontine angle in relation to trigeminal nerve
			Process posteriorly to right m. psoas[b]
			Anteriorly to L5/S1, right side[b]
			In the right neuroforamina L4/L5[b]
		21	Left neuroforamina C6/C7[b]
			Intraspinal process, probably intradural and extramedullary, posterior to C7/Th1 disc[c]
			Left to sternum

[a]Tentative diagnosis: neurofibroma.
[b]Tentative diagnosis: schwannoma.
[c]Tentative diagnosis: meningioma.

14. The benign tumors include at least three neurofibromas (none plexiform), all of which resected, and five tumors thought to be schwannomas based on MRI. The latest atypical neurofibromatous neoplasm of uncertain biological potential (ANNUBP) was examined by NGS analysis (for details regarding NGS analysis, view the Table 4 footnote), showing heterozygote deletion of *CDKN2A/B* and small indels in both *NF1* and *CDKN2A* causing truncating variants (for specific variants, view Table 4). An overview of malignant, premalignant, and benign tumors is presented in Tables 2 and 3.

At present, the proband is receiving symptomatic treatment and frequent imaging of the high-grade astrocytoma with piloid features and the multiple benign peripheral nerve sheath tumors. In addition, a surveillance program comprising of quarterly MRI of the neuroaxis and annually melanoma screening has been followed since the age of 16 yr.

Genomic Analyses

At age 15, after diagnosis of the anaplastic pleomorphic xanthoastrocytoma, genomic analysis was performed. Exome sequencing did not show any pathogenic variants. A CytoScan HD SNP array found a heterozygous germline deletion on Chromosome 9p21.3, including *CDKN2A*, *CDKN2B*, and the *IFN* gene family. Multiplex ligation-dependent probe amplification (MLPA) analysis and parental testing confirmed a de novo *CDKN2A/CDKN2B* deletion (Østrup et al. 2018).

Table 4. Overview of germline deletion and somatic variants in our proband

Germline/somatic (tumor)	Gene(s)	Chromosome	HGVS DNA reference	HGVS protein reference	Variant type	Predicted effect	dbSNP/dbVar ID	Genotype
Germline	[a]	9p21.3	seq(GRCh37) del(9)(p21.3) NC_00009.11:g.20657836-22353823del	N/A	Deletion	Pathogenic	N/A	Heterozygous
Somatic (APXA)	*BRAF*	7q34	NM_004333.4: c.1799T > A	p.Val600Glu	Missense	Pathogenic	N/A	N/A
Somatic (APXA)	*SP140*	2q37.1	NM_007237.4: c.1994G > C	p.Arg665Thr	Missense	N/A	N/A	N/A
Somatic (APXA)	*ALDH5A1*	6p22.3	NM_001080.3: c.838_839delAT	p.Ile280fs[a]37	Frameshift	N/A	N/A	N/A
Somatic (APXA)	*SCUBE2*	11p15.4	NM_020974.2: c.1558G > A	p.Val520Ile	Missense	N/A	N/A	N/A
Somatic (APXA)	*GRP*	18q21.32	NM_002091.3: c.239C > T	p.Ala80Val	Missense	N/A	N/A	N/A
Somatic (APXA)	*WDR62*	19q13.12	NM_173636.4: c.1917_1918delCCinsGT	p.Gln640[a]	In-frame	N/A	N/A	N/A
Somatic (high-grade astrocytoma with piloid features)	*NF1*	17q11.2	NM_000267.3:c.6789_6792del	p.Tyr2264Thrfs[a]5	Frameshift	Pathogenic	dbSNP: rs863224836	N/A
Somatic (high-grade astrocytoma with piloid features)	*NF1*	17q11.2	NM_000267.3:c.1393-1G > A	p.?	Splice acceptor	Likely pathogenic	dbSNP: rs1131691131	N/A
Somatic (latest ANNUBP)	*CDKN2A*	9p21.3	c.191_212delinsCGTGG	p.Leu64fs[a]50	Frameshift	N/A	N/A	N/A
Somatic (latest ANNUBP)	*NF1*	17q11.2	c.1026_1035del	p.Ile342fs[a]31	Frameshift	N/A	N/A	N/A

Somatic sequence data of biopsy of high-grade astrocytoma with piloid features:
NGS analysis was performed using a neuropanel covering hotspots in the following genes: *BRAF, FGFR1, H3F3A, Hist1H3B, Hist1H3C, IDH1, IDH2, PIK3CA, PIK3R1, MET, NRAS, SMO*, and *TERT* promoter. The panel covers the whole coding sequence of the following genes: *ATRX, CDKN2A, CDKN2B, CDKN2C, CIC, EGFR, FUBP1, NF1, NF2, NOTCH1, PTEN, RB1*, and *TP53*. Further, there was an examination of codeletion of 1p and 19q. Sensitivity of mutations in the analysis is 5% tumor cell nuclei.
Somatic sequence data of resection of the latest atypical neurofibromatous neoplasm of uncertain biological potential (ANNUBP):
Next-generation sequencing mutation analysis and copy-number variation analysis was performed using a neuropanel covering the following genes: *ATRX*^, *BRAF**, *CDKN2A*"^, *CDKN2B*"^, *CDKN2C*^, *CIC*^, *EGFR*"^, *FGFR1**, *FUBP1*^, *H3F3A**, *Hist1H3B**, *Hist1H3C**, *IDH1**, *IDH2**, *MET**, *NF1*^, *NF2*^, *NOTCH1*^, *NRAS**, *PIK3CA**, *PIK3R1**, *PTEN*^, *RB1*^, *SMO**, *TERT* promoter*, and *TP53*^. Further, there was an examination of 1p monosomy and codeletion of 1p and 19q. Sensitivity of mutations in the analysis is 5% tumor cell nuclei. (*) The analysis covers most frequent hotspot mutations, (") the analysis covers copy-number variants, (^) the analysis covers the whole coding sequence.
[a]*CDKN2A, CDKN2B, CDKN2A-AS1, CDKN2B-AS1, ERVFRD-3, FOCAD, FOCAD-AS1, HACD4, IFNA1, IFNA10, IFNA13, IFNA14, IFNA16, IFNA17, IFNA2, IFNA21, IFNA22P, IFNA4, IFNA5, IFNA6, IFNA7, IFNA8, IFNB1, IFNE, IFNW1, IFNWP15, IFNWP18, IFNWP2, IFNWP5, IFNWP9, KHSRPP1, KLHL9, MIR31, MIR31HG, MIR491, MTAP, TUBB8P1, UBA52P6*.

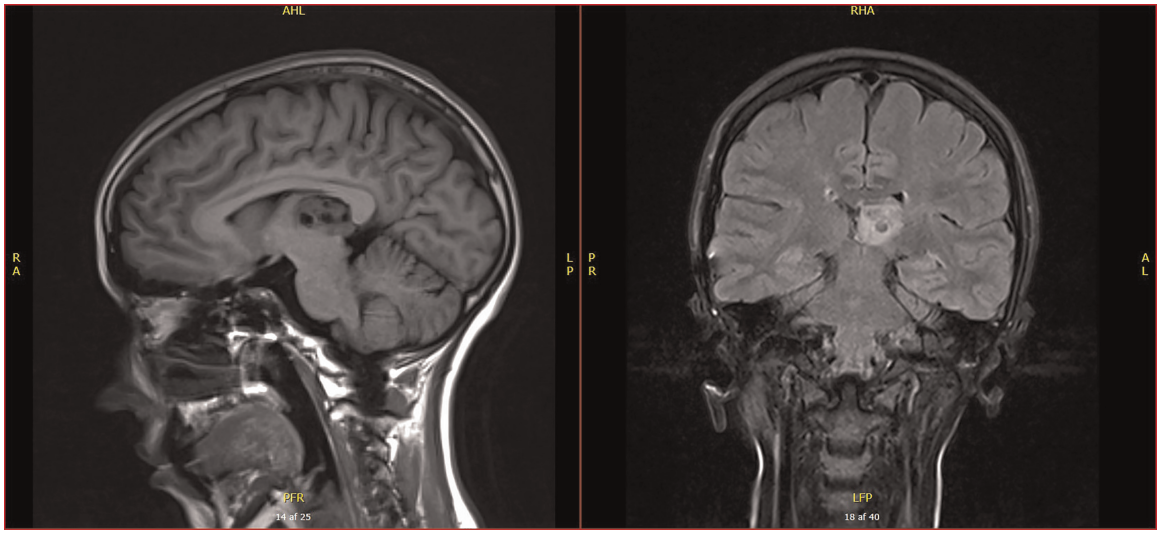

Figure 1. Latest magnetic resonance imaging of the high-grade astrocytoma with piloid features, showing stable tumor size.

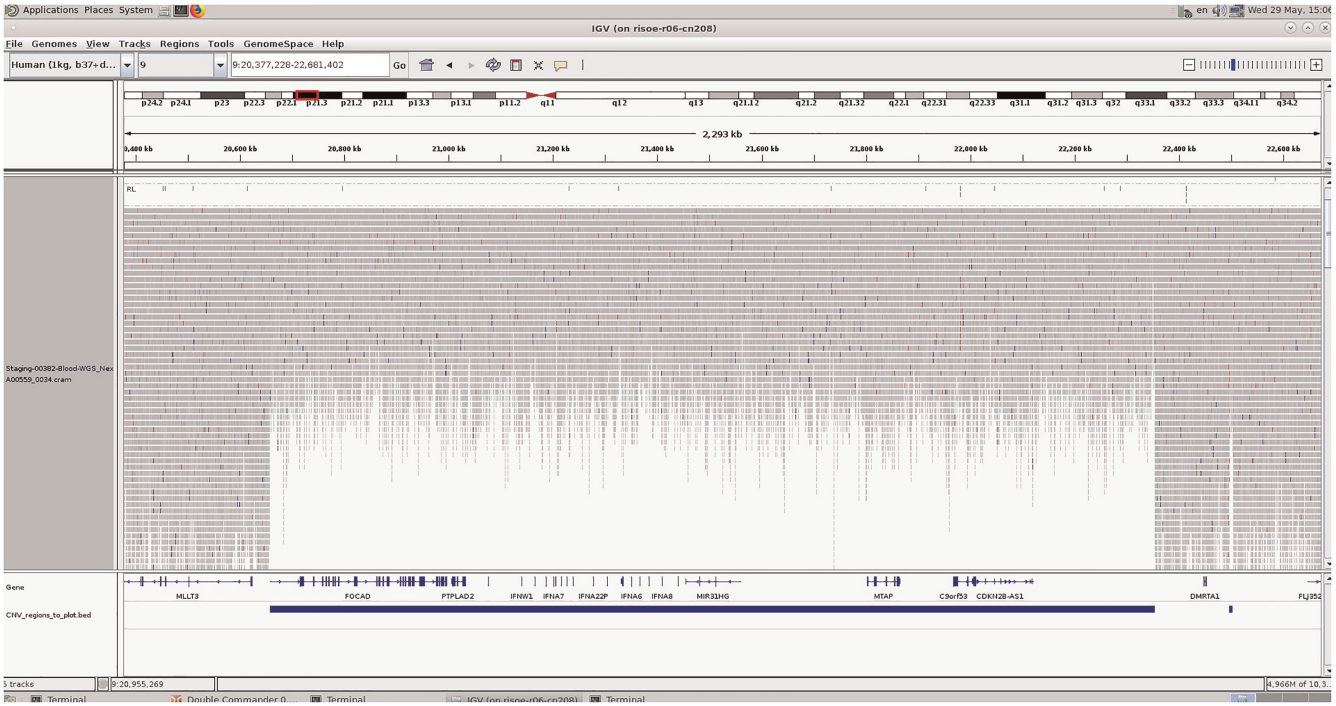

Figure 2. Whole-genome sequencing demonstrating the heterozygous germline deletion on Chromosome 9p21.3 containing *CDKN2A* and *CDKN2B*.

At age 19, the proband was referred to genetic counseling and offered WGS as part of a research project, STAGING (Byrjalsen et al. 2020). A written consent for publication was obtained in the STAGING project. WGS mapped the deletion and determined the size to be 1.7 MB (seq(GRCh37) del(9)(p21.3) NC_00009.11:g.20657836-22353823del), further including the genes *FOCAD*, *MTAP*, and *CDKN2B-AS1* (Table 4; Fig. 2). For determination of the exact breakpoints, fine mapping of the deletion break points is necessary. No additional known pathogenic variants in genes suspected of cancer predisposition syndrome (CPS) were identified.

DISCUSSION

In a patient with a germline microdeletion and a severe cancer predisposition, difficulties arise regarding evaluating the contribution of the individual genes, and the manifestations could be suggestive of an additive genetic effect or a contiguous gene deletion syndrome, meaning that tumor proneness possibly could relate to the size of the deletion.

In addition to *CDKN2A* and *CDKN2B*, the deletion in our proband involved the genes *FOCAD*, *CDKN2B-AS1, MTAP*, and the *IFN* gene cluster. However, these genes do not yet have a well-described role in terms of cancer predisposition. *FOCAD* encodes the tumor suppressor focadhesin, and one study has found germline deletions in the *FOCAD* gene to be associated to colorectal cancer (Weren et al. 2015). *CDKN2B-AS1*, previously designated *ANRIL*, is an antisense noncoding RNA partially located within the *CDKN2A–CDKN2B* locus suspected of suppressing the expression of *CDKN2A* and *CDKN2B* (Visel et al. 2010; Yap et al. 2010; Kotake et al. 2011). In a family-based association study by Pasmant et al., a SNP rs2151280 within *CDKN2B-AS1* was found to be associated with the number of plexiform neurofibromas (PNFs) in NF1 patients (Pasmant et al. 2011). However, further studies are necessary before a significance of *CDKN2B-AS1* deletion in terms of tumor predisposition can be established.

To our knowledge, neither the *IFN* gene cluster nor *MTAP* is known to cause cancer predisposition. However, Linsley et al. finds that homozygous deletion of the *IFN* gene cluster may contribute to reduced tumor destruction by the immune system (Linsley et al. 2014), thus potentially leading to a worse prognosis. Exploring the role of *MTAP*, a gene encoding a key enzyme in the adenine and methionine salvage pathway, two reports have shown that cancer cells with homozygously deleted *MTAP* can be sensitive to PRMT5 inhibition, which may be at potential therapeutic strategy (Kryukov et al. 2016; Mavrakis et al. 2016). Further, a report by Camacho-Vanegas et al. (2012) found that germline splice variants of *MTAP* can result in a distinctive clinical phenotype with diaphyseal medullary stenosis and increased risk of malignant fibrous histiocytoma, and has suggested that *MTAP* function as a tumor suppressor.

A total of six families describing germline deletion of the entire *CDKN2A/CDKN2B* locus have previously been described, comprising 20 confirmed carriers with a total of at least 32 malignant or premalignant cancers and 13 benign tumors. The cases are presented in Table 1 according to the size of the deletion. A large span is seen in age at presentation and severity of cancer manifestation in these cases, possibly reflecting differences in deletion size and thus supportive of the contiguous gene deletion syndrome. Regarding co-deleted genes, the report by Frigerio et al. (2014) describing a girl with a severe tumor manifestation and the largest well-determined deletion (2.1 Mb), involves *FOCAD*, *MTAP*, the *IFN* gene cluster, and as well partly *CDKN2B-AS1*. The case by Baker et al. (2016) describes a deletion involving *MTAP*, and the approximate coordinates of the deletion suggest affected gene

function of *FOCAD* as well. Similarly, the approximate coordinates of the deletion in the case by Chan et al. (2017) suggests deletion of *MTAP* (Chan et al. 2017).

The analysis of a potential contiguous gene deletion syndrome is limited by the small number of cases, by available clinical data, and by the fact that only one previous study (Chan et al. 2016) has performed extensive sequencing by WGS and thereby excluded alterations in additional cancer predisposition genes. Additional cancer predisposition alterations may be present in the case by Petty et al. (1993) as the *CDKN2A/CDKN2B* deletion was the result of an unbalanced translocation between Chromosome 5p and 9p. Further studies will be necessary to evaluate the possibility of a contiguous gene deletion syndrome.

Regarding somatic *NF1* variants, the high-grade astrocytoma with piloid features had two somatic *NF1* variants, as previously mentioned, none of which identified germline including screening for mosaicism. Analysis of the APXA with whole-exome sequencing (WES) did not show *NF1* alterations. None of the additional tumors has been analyzed. An increased propensity for somatic *NF1* alterations when a germline *CDKN2A* ($p14^{ARF}$) alteration is present, has previously been suggested (Rhodes et al. 2019), but further investigations have to be performed to confirm this interaction. However, both gliomas and one of the atypical neurofibromas have shown homozygous loss of *CDKN2A/CDKN2B*, which suggests *CDKN2A/CDKN2B* as driving for tumor development in the neural system tumors as well as the patient's tumors not typical for *NF1*.

Potential consequences of cancer treatment must be discussed as well. In our case, three of the cancers have been treated with alkylating chemotherapeutics, beginning in the treatment of the proband's very first cancer at age 8 yr. Alkylating chemotherapeutics are known to induce alterations in DNA, and similarly radiation therapy can increase risk of cancer in the radiation field. This patient has received radiation therapy to the neck and rhinopharynx in the treatment of the lymphoepithelial carcinoma (2 Gy × 34) and in treatment of the latest tumor, the high-grade astrocytoma with piloid features (54 Gy). Thus, chemotherapy and radiation therapy could also have contributed to subsequent tumor development.

Multiple pediatric cancer predisposition syndromes have recommended surveillance protocols (Frebourg et al. 2020; Durno et al. 2021). Interestingly, two of the six malignant tumors (the low-grade myofibroblastic sarcoma and the high-grade astrocytoma with piloid features) and the relapse of APXA in the patient presented were identified asymptomatically. Early asymptomatic diagnosis may be vitally important for patients at high risk of multiple cancers. When purely surgical cures are possible it ensures not just decreased mortality and morbidity, but also that dosage-limited therapies such as radiation and less toxic chemotherapy are still options for subsequent, harder-to-treat cancers. In addition, surveillance can prevent malignancy by surgical removal of premalignant tumors.

Difficulties arise in establishing recommendations regarding surveillance for patients with *CDKN2A–CDKN2B* microdeletions, as we are limited by the rarity of this syndrome and the large span in age, cancer type, and severity between the cases. In our case, the patient fulfills the Chompret criteria for LFS. Thus, a surveillance protocol resembling LFS protocols, such as the Toronto protocol (Villani et al. 2016), should be considered. However, it should be noted that LFS surveillance is recommended for confirmed germline *TP53* variant carriers. Although optimal strategies remain unknown, we encourage evaluation of each patient's clinical presentation, family history, and the deletion when planning a surveillance protocol.

In summary, this case illustrates that pediatric cancer patients with a phenotype resembling LFS should be offered additional extensive genetic evaluation if no germline *TP53* variant is identified, to exclude structural alterations or variants in other CPS genes. Similarly, as most of the presented cases of *CDKN2A/CDKN2B* germline deletions have reported nerve sheath tumors and/or gliomas, including our own case, the *CDKN2A/CDKN2B* locus should

also be assessed in patients with neural system tumors without pathogenic variants in *NF1*, *NF2*, *LZTR1*, and *SMARCB1*.

By identifying such pathogenic variants, affected patients will be available for targeted surveillance regimens, which potentially can identify any additional tumors at an early and treatable stage. Further, identification permits presymptomatic testing of relatives at risk, as well as prenatal diagnosis.

METHODS

Methods of WGS (and RNA sequencing) follow the STAGING project and can be viewed in detail in the study by Byrjalsen et al. (2020). Further, details of exome sequencing, the CytoScan HD SNP array, and MLPA analysis can be viewed in the study by Østrup et al. (2018).

The cancer panel–specific coverage in WGS is more than 20×: 98.53%

ADDITIONAL INFORMATION

Data Deposition and Access

Consent was not given for deposition of the data raw file of WGS data or of exome sequencing of APXA. Germline data are deposited in DECIPHER (https://www.deciphergenomics.org/) and can be found under accession number 480874.

Ethics Statement

Written patient consent was obtained. The project has been approved by the regional ethics committee (H-15016782).

Acknowledgments

We thank our patient for contributing to this study.

Author Contributions

K.W. provided genetic counseling and obtained informed consent. K.W. and M.R.J. wrote the manuscript. M.B. imaged the WGS data. M.R.J. provided the clinical image. All authors contributed to revision of the manuscript and approved the final manuscript and its submission to *Cold Spring Harbor Molecular Case Studies*.

Competing Interest Statement

The authors have declared no competing interest.

Referees

D Gareth Evans
Maria-Isabel Achatz
Anonymous

Received December 7, 2021; accepted in revised form April 1, 2022.

Funding

This study was financially supported by the Independent Research Fund Denmark (M.R.J.; https://dff.dk/) and the European Union's Interregional Öresund-Kattegat-Skagerrak grant (https://interreg-oks.eu/). This work is part of the nationwide research program Childhood Oncology Network Targeting Research, Organization & Life expectancy (CONTROL) and supported by the Danish Cancer Society (R-257-A14720), the Danish Childhood Cancer Foundation (2019-5934 and 2020-5769), and the NEYE foundation. This work is part of Interregional Childhood Oncology Precision Medicine Exploration (iCOPE), a cross-Oresund collaboration between University Hospital Copenhagen, Rigshospitalet, Lund University, Region Skåne, and Technical University Denmark (DTU), supported by the European Regional Development Fund.

REFERENCES

Bahuau M, Vidaud D, Jenkins RB, Bièche I, Kimmel DW, Assouline B, Smith JS, Alderete B, Cayuela JM, Harpey JP, et al. 1998. Germ-line deletion involving the *INK4* locus in familial proneness to melanoma and nervous system tumors. *Cancer Res* **58:** 2298–2303.

Baker MJ, Goldstein AM, Gordon PL, Harbaugh KS, Mackley HB, Glantz MJ, Drabick JJ. 2016. An interstitial deletion within 9p21.3 and extending beyond *CDKN2A* predisposes to melanoma, neural system tumours and possible haematological malignancies. *J Med Genet* **53:** 721–727. doi:10.1136/jmedgenet-2015-103446

Byrjalsen A, Hansen TVO, Stoltze UK, Mehrjouy MM, Barnkob NM, Hjalgrim LL, Mathiasen R, Lautrup CK, Gregersen PA, Hasle H, et al. 2020. Nationwide germline whole genome sequencing of 198 consecutive pediatric cancer patients reveals a high frequency of cancer prone syndromes. *PLoS Genet* **16:** 1–24. doi:10.1371/JOURNAL.PGEN.1009231

Camacho-Vanegas O, Camacho SC, Till J, Miranda-Lorenzo I, Terzo E, Ramirez MC, Schramm V, Cordovano G, Watts G, Mehta S, et al. 2012. Primate genome gain and loss: a bone dysplasia, muscular dystrophy, and bone cancer syndrome resulting from mutated retroviral-derived MTAP transcripts. *Am J Hum Genet* **90:** 614–627. doi:10.1016/j.ajhg.2012.02.024

Chan SH, Lim WK, Michalski ST, Lim JQ, Ishak NDB, Met-Domestici M, Young CNC, Vikstrom K, Esplin ED, Fulbright J, et al. 2016. Germline hemizygous deletion of *CDKN2A-CDKN2B* locus in a patient presenting with Li–Fraumeni syndrome. *NPJ Genomic Med* **1:** 1–6. doi:10.1038/npjgenmed.2016.15

Chan AK, Han SJ, Choy W, Beleford D, Aghi MK, Berger MS, Shieh JT, Bollen AW, Perry A, Phillips JJ, et al. 2017. Familial melanoma-astrocytoma syndrome: synchronous diffuse astrocytoma and pleomorphic xanthoastrocytoma in a patient with germline CDKN2A/B deletion and a significant family history. *Clin Neuropathol* **36:** 213–221. doi:10.5414/NP301022

Durno C, Ercan AB, Bianchi V, Edwards M, Aronson M, Galati M, Atenafu EG, Abebe-Campino G, Al-Battashi A, Alharbi M, et al. 2021. Survival benefit for individuals with constitutional mismatch repair deficiency undergoing surveillance. *J Clin Oncol* **39:** 2779–2790. doi:10.1200/JCO.20.02636

Frebourg T, Bajalica Lagercrantz S, Oliveira C, Magenheim R, Evans DG, Hoogerbrugge N, Ligtenberg M, Kets M, Oostenbrink R, Sijmons R, et al. 2020. Guidelines for the Li–Fraumeni and heritable *TP53*-related cancer syndromes. *Eur J Hum Genet* **28:** 1379–1386. doi:10.1038/s41431-020-0638-4

Frigerio S, Disciglio V, Manoukian S, Peissel B, Della Torre G, Maurichi A, Collini P, Pasini B, Gotti G, Ferrari A, et al. 2014. A large de novo 9p21.3 deletion in a girl affected by astrocytoma and multiple melanoma. *BMC Med Genet* **15:** 1–6. doi:10.1186/1471-2350-15-59

Jafri M, Wake NC, Ascher DB, Pires DE V, Gentle D, Morris MR, Rattenberry E, Simpson MA, Trembath RC, Weber A, et al. 2015. Germline mutations in the *CDKN2B* tumor suppressor gene predispose to renal cell carcinoma. *Cancer Discov* **5:** 723–729. doi:10.1158/2159-8290.CD-14-1096

Kotake Y, Nakagawa T, Kitagawa K, Suzuki S, Liu N, Kitagawa M, Xiong Y. 2011. Long non-coding RNA *ANRIL* is required for the PRC2 recruitment to and silencing of $P15^{INK4B}$ tumor suppressor gene. *Oncogene* **30:** 1956–1962. doi:10.1038/onc.2010.568

Kryukov GV, Wilson FH, Ruth JR, Paulk J, Tsherniak A, Marlow SE, Vazquez F, Weir BA, Fitzgerald ME, Tanaka M, et al. 2016. *MTAP* deletion confers enhanced dependency on the PRMT5 arginine methyltransferase in cancer cells. *Science* **351:** 1214–1218. doi:10.1126/science.aad5214

Linsley PS, Speake C, Whalen E, Chaussabel D. 2014. Copy number loss of the interferon gene cluster in melanomas is linked to reduced T cell infiltrate and poor patient prognosis. *PLoS ONE* **9:** e109760. doi:10.1371/journal.pone.0109760

Mavrakis KJ, Robert McDonald E III, Schlabach MR, Billy E, Hoffman GR, deWeck A, Ruddy DA, Venkatesan K, Yu J, McAllister G, et al. 2016. Disordered methionine metabolism in MTAP/CDKN2A-deleted cancers leads to dependence on PRMT5. *Science* **351:** 1208–1213. doi:10.1126/science.aad5944

Østrup O, Nysom K, Scheie D, Schmidt AY, Mathiasen R, Hjalgrim LL, Olsen TE, Skjøth-Rasmussen J, Henriksen BM, Nielsen FC, et al. 2018. Importance of comprehensive molecular profiling for clinical outcome in children with recurrent cancer. *Front Pediatr* **6:** 114. doi:10.3389/fped.2018.00114

Pasmant E, Laurendeau I, Héron D, Vidaud M, Vidaud D, Bièche I. 2007. Characterization of a germ-line deletion, including the entire *INK4/ARF* locus, in a melanoma-neural system tumor family: identification of *ANRIL*, an antisense noncoding RNA whose expression coclusters with *ARF*. *Cancer Res* **67:** 3963–3969. doi:10.1158/0008-5472.CAN-06-2004

Pasmant E, Sabbagh A, Masliah-Planchon J, Ortonne N, Laurendeau I, Melin L, Ferkal S, Hernandez L, Leroy K, Valeyrie-Allanore L, et al. 2011. Role of noncoding RNA ANRIL in genesis of plexiform neurofibromas in neurofibromatosis type 1. *J Natl Cancer Inst* **103:** 1713–1722. doi:10.1093/jnci/djr416

Petty EM, Gibson LH, Fountain JW, Bolognia JL, Yang-Feng TL, Housman DE, Bale AE. 1993. Molecular definition of a Chromosome 9p21 germ-line deletion in a woman with multiple melanomas and a plexiform neurofibroma: implications for 9p tumor-suppressor gene(s). *Am J Hum Genet* **53:** 96–104.

Rhodes SD, He Y, Smith A, Jiang L, Lu Q, Mund J, Li X, Bessler W, Qian S, Dyer W, et al. 2019. *Cdkn2a (Arf)* loss drives NF1-associated atypical neurofibroma and malignant transformation. *Hum Mol Genet* **28:** 2752–2762. doi:10.1093/hmg/ddz095

Villani A, Shore A, Wasserman JD, Stephens D, Kim RH, Druker H, Gallinger B, Naumer A, Kohlmann W, Novokmet A, et al. 2016. Biochemical and imaging surveillance in germline *TP53* mutation carriers with Li–Fraumeni syndrome: 11 year follow-up of a prospective observational study. *Lancet Oncol* **17:** 1295–1305. doi:10.1016/S1470-2045(16)30249-2

Visel A, Zhu Y, May D, Afzal V, Gong E, Attanasio C, Blow MJ, Cohen JC, Rubin EM, Pennacchio LA. 2010. Targeted deletion of the 9p21 non-coding coronary artery disease risk interval in mice. *Nature* **464:** 409–412. doi:10.1038/nature08801

Weren RDA, Venkatachalam R, Cazier JB, Farin HF, Kets CM, de Voer RM, Vreede L, Verwiel ETP, van Asseldonk M, Kamping EJ, et al. 2015. Germline deletions in the tumour suppressor gene *FOCAD* are associated with polyposis and colorectal cancer development. *J Pathol* **236:** 155–164. doi:10.1002/path.4520

Yap KL, Li S, Muñoz-Cabello AM, Raguz S, Zeng L, Mujtaba S, Gil J, Walsh MJ, Zhou MM. 2010. Molecular interplay of the noncoding RNA *ANRIL* and methylated histone H3 lysine 27 by Polycomb CBX7 in transcriptional silencing of *INK4a*. *Mol Cell* **38:** 662–674. doi:10.1016/j.molcel.2010.03.021